Journal of Inorganic Biochemistry 158 (2016) 70–76

Contents lists available at ScienceDirect

Journal of Inorganic Biochemistry

journal homepage: www.elsevier.com/locate/jinorgbio

Sequence proximity between Cu(II) and Cu(I) binding sites of human copper transporter 1 model peptides defines reactivity with ascorbate and O_2

Stefanie Schwab [a], Jason Shearer [b], Steven E. Conklin [c], Bruno Alies [c], Kathryn L. Haas [a,*]

[a] Department of Chemistry and Physics, Saint Mary's College, Notre Dame, IN, USA
[b] Department of Chemistry, University of Nevada, Reno, USA
[c] Department of Chemistry, Duke University, Durham, NC, USA

ARTICLE INFO

Article history:
Received 28 July 2015
Received in revised form 25 November 2015
Accepted 28 December 2015
Available online 30 December 2015

Keywords:
Copper transport
ATCUN
bis–His
Ctr1
EXAFS
Reductase

ABSTRACT

The critical nature of the copper transporter 1 (Ctr1) in human health has spurred investigation of Ctr1 structure and function. Ctr1 specifically transports Cu(I), the reduced form of copper, across the plasma membrane. Thus, extracellular Cu(II) must be reduced prior to transport. Unlike yeast Ctr1, mammalian Ctr1 does not rely on any known mammalian reductase. Previous spectroscopic studies of model peptides indicate that human Ctr1 could serve as both copper reductase and transporter. Ctr1 peptides bind Cu(II) at an amino terminal high-affinity Cu(II), Ni(II) ATCUN site. Ascorbate-dependent reduction of the Cu(II)–ATCUN complex is possible by virtue of an adjacent HH (*bis*–His), as this *bis*–His motif and one methionine ligand constitute a high affinity Ctr1 Cu(I) binding site. Here, we synthetically varied the distance between the ATCUN and *bis*–His motifs in a series of peptides based on the human Ctr1 amino terminal, with the general sequence $MDHA_nHHMGMSYMDS$, where $n = 0$–4. We tested the ability of each peptide to reduce Cu(II) with ascorbate and stabilize Cu(I) under ambient conditions (20% O_2). This study reveals that significant differences in coordination structure and chemical behavior with ascorbate and O_2 result from changes in the sequence proximity of ATCUN and *bis*–His. Peptides that deviate from the native Ctr1 pattern were less effective at forming stable Cu(I)–peptide complexes and/or resulted in O_2-dependent oxidative damage to the peptide.

1. Introduction

The copper transporter 1 protein (Ctr1), a member of the Ctr family of conserved transmembrane copper transport proteins, is essential to eukaryotic life [1,2]. Ctr1 is principally responsible for acquiring extracellular Cu and transporting it through the plasma membrane into the cellular cytoplasm [1]. Cellular copper acquisition, and thus Ctr1, is required for sustaining the function of essential cuproenzymes, including copper–zinc superoxide dismutase, cytochrome-c oxidase, lysyl oxidase, ceruloplasmin, dopamine β-hydroxylase, tyrosinase, peptidylglycine monooxygenase, clotting factors V and VIII, angiogenin, and hephaestin [3,4]. Ctr1 homotrimerizes in the plasma membrane to form a Cu(I)-selective pore. Each Ctr1 monomer has three transmembrane domains, an intracellular carboxy terminus, and an extracellular amino terminus. The extracellular, amino terminal domain is largely unstructured, and is presumably responsible for binding to copper and increasing its local concentration at the extracellular side of the Ctr1 pore so that Cu(I) is transported passively down its concentration gradient.

Recent evidence demonstrates that the extracellular copper carrier, human serum albumin, can directly interact with the Ctr1 amino terminus [5] and can transfer Cu(II) to the extracellular domain of human Ctr1 [6]. The extracellular domain of human Ctr1 binds to Cu(II) with an amino terminal high affinity Cu(II), Ni(II) (ATCUN) binding site, comprised of a histidine in the third position from the free amino terminus [7–9]. A similar ATCUN motif comprises the high-affinity Cu(II)-binding site of human serum albumin.

Extracellular interaction between Cu(II) and Ctr1 is unique to humans and other metazoans, which contain high-affinity copper-binding histidine-rich motifs in their extracellular domains [7,10]. The presence of ATCUN and other histidine-rich motifs enables both high-affinity Cu(II)–Ctr1 interactions and an increased Cu(I)-binding affinity to human Ctr1 relative to Ctr1 found in other organisms. For example, it has been found that human Ctr1 model peptide has a Cu(I) binding affinity that is by six orders of magnitude greater than that of yeast Ctr1, which contain only Cu(I) specific, methionine-rich Cu(I) binding motifs (i.e. Mets motifs) [11,12].

Despite its high affinity for Cu(II), human Ctr1 specifically transports Cu(I) across the plasma membrane. Thus after receiving Cu(II) from human serum albumin, extracellular copper must be reduced to Cu(I) before passing though the human Ctr1 pore [1,13–16]. The

* Corresponding author.
E-mail address: khaas@saintmarys.edu (K.L. Haas).

http://dx.doi.org/10.1016/j.jinorgbio.2015.12.021
0162-0134/

mechanism of Cu(II) reduction is unclear in mammalian cells. Unlike yeast Ctr1, which requires the action of Fre1/2 iron–copper reductases [13,17], human Ctr1 has no known dependence on a mammalian reductase. However, recent work with model peptides of the first fourteen amino acids of the N-terminal Cu acquisition domain of human Ctr1 (Ctr1-14 peptide) suggests that human Ctr1 may coordinate to Cu(II) in a manner allowing for its reduction by weak biological reductants, like ascorbate (vitamin C) [7]. The hypothesis that Ctr1 may serve as a copper reductase in the presence of ascorbate is further supported by biological evidence. For example, it is well known that the rate of cellular copper uptake by Ctr1 and the total cellular copper load increase significantly in the presence of ascorbate [14,18,19].

The extracellular Cu acquisition domain of human Ctr1 possesses two adjacent histidines (*bis*–His) in the fifth and sixth positions from the amino terminus. In the native sequence of human Ctr1, the *bis*–His motif is one amino acid away from the Cu(II)-binding ATCUN motif. This *bis*–His motif provides a high-affinity Cu(I)-binding site, which has recently been characterized in the Ctr1-14 peptide [20]. The Ctr1-14 peptide contains an ATCUN motif, a *bis*–His motif, and one of the two human Ctr1 Mets motifs. When Cu(II) is bound to the ATCUN site of Ctr1-14, the *bis*–His motif facilitates the reduction of copper by ascorbate, and forms a relatively stable Cu(I)–peptide complexes under ambient conditions (approximately 20% O_2) [7]. The pseudo-tetrahedral 2N(imidazole), 1S(Met), 1O(backbone) Cu(I) coordination of the *bis*–His and one Met reported for Ctr1-14 is proposed to be an intermediate in Ctr1 Cu transport, following Cu(II) reduction, and preceding 3S(Met) coordination in the Ctr1 pore [16,20].

The reduction of copper and stabilization of Cu(I) in the presence of extracellular O_2 may be a critical function of human Ctr1 in certain tissues where extracellular O_2 is abundant. Although other Cu(II)–ATCUN peptides are known to catalyze the copper-dependent oxidation of ascorbate, ATCUN-only peptides do not form stable Cu(I)–peptide species in the presence of oxygen [21]. In the case of Ctr1-14, the *bis*–His sequence adjacent to the Cu(II)–ATCUN site provides a high-affinity Cu(I) binding site which presumably increases the potential of the $Cu^{2+/1+}$ cycle, allowing Cu(II) to be reduced by ascorbate and stabilized as Cu(I)–peptide species [7].

The Ctr1 ATCUN and *bis*–His motifs are conserved across many metazoan species; however, the sequence proximity of ATCUN and *bis*–His is variable among these species. Some mammalian proteins also contain ATCUN and *bis*–His sequences in close proximity. For example, the human salivary Histatin 5 peptide and the truncated Alzheimer's disease Aβ4-42 peptide each contains an ATCUN and *bis*–His motif separated by three and six amino acids, respectively [22–25]. ATCUN and *bis*–His motifs have been individually characterized in other systems, yet the interplay of ATCUN and *bis*–His motifs in controlling copper redox chemistry has not been previously investigated.

What, if any, role might the proximity of the ATCUN and *bis*–His site play on the copper redox chemistry of Ctr1 model peptides? This question prompted us to investigate how the proximity of the ATCUN and *bis*–His motifs might affect the previously-demonstrated reduction of Cu(II)–Ctr1-14 complexes with ascorbic acid under ambient conditions [7]. To determine the role, if any, that the proximity of the ATCUN and *bis*–His site play on the redox chemistry of copper we examined a number of peptides based on the native Ctr1-14 peptide sequence. Presented herein, is a series of peptides having the general formula $MDHA_nHHMGMSYMDS$ (designated $CtrA_n$; n = 0–4, Table 1). We examined each peptide's ability to reduce Cu(II) to Cu(I), and subsequently stabilize Cu(I) in the presence of ascorbate under ambient conditions (20% O_2). This study reveals that significant differences in Cu(I) coordination structure result from changes in the relative proximity of the ATCUN and *bis*–His. These changes culminate in a spectrum of chemical behavior with ascorbate and O_2. We find that peptides that retain the native one-amino acid spacing between ATCUN and *bis*–His facilitate reduction and protect the peptide against oxidative damage. Peptides which deviate from the native Ctr1 pattern lose the ability to facilitate copper reduction and/or are subjected to O_2-dependent oxidative damage upon reaction with ascorbate.

Table 1
Ctr1-14 model peptide and variants with serial increase in the number of Ala (A) between the Cu(II)-binding ATCUN site and the *bis*–His site.

Peptide name	Amino acid sequence
Ctr1-14	MD**H**S**HH**MGMSYMDS
$CtrA_0$	MD**HHH**MGMSYMDS
$CtrA_1$	MD**H**A**HH**MGMSYMDS
$CtrA_2$	MD**H**AA**HH**MGMSYMDS
$CtrA_3$	MD**H**AAA**HH**MGMSYMDS
$CtrA_4$	MD**H**AAAA**HH**MGMSYMDS

Histidines (H) are bolded. ATCUN and *bis*–His motifs are underlined.

2. Experimental section

2.1. Peptide synthesis and purification

Model peptides based on the first fourteen amino acids of the extracellular N-terminal domain of Ctr1 (Ctr1-14: MDHSHHMGMSYMDS, and $CtrA_n$ series: $MDHA_nHHMGMSYMDS$, where $n = 0–4$) were synthesized on a Protein Technologies PS3 automated peptide synthesizer on Rink Amide MBHA Low Loaded Resin (Protein Technologies) on a 0.2 mmol scale. Couplings of standard 9-fluoromethoxy-carbonyl (Fmoc)-protected amino acids (Chem-Impex) were achieved using HCTU (O-(6-chlorobenzotriazol-1-yl)-N,N,N',N'-tetramethyluronium hexafluorophosphate, Protein Technologies) in the presence of NMM (N-methylmorpholine, Sigma-Aldrich) in DMF (N,N-dimethylformamide, Protein Technologies) for 10 min cycles. Fmoc deprotection was achieved with 20% piperidine in DMF. The N-terminus was left as the free amine. Side chain deprotection and peptide cleavage from the resin were achieved by treating the resin-bound peptide with 7–10 mL of a solution of 95% trifluoroacetic acid (TFA), 2.5% ethane dithiol (EDT), and 2.5% triisopropylsilane (TIS, Sigma-Aldrich) for four hours under N_2. An additional 150 μL of EDT and 130 μL of bromotrimethylsilane (TMSBr, Sigma-Aldrich) were added during the last 30 min to minimize methionine oxidation and to scavenge carbocations. A stream of N_2 was used to evaporate TFA to a volume of about 2 mL. Peptides were precipitated and washed three times with 10 mL diethyl ether (Sigma-Aldrich). Peptides were air-dried and then purified by preparatory reverse-phase HPLC on a YMC C18 Column with a linear gradient from 7–97% acetonitrile in water, with 0.1% TFA. Purity was validated to >95% by analytical HPLC, and the mass of the peptide was confirmed by ESI-MS. Ctr1-14 peptide: Calculated *m*/*z*, where $z = 2$, (Peptide + $2H^+$) 818.23. Found *m*/*z* (Peptide + $2H^+$) 818.49.

2.2. Preparation of stock solutions

Stock solutions of peptides were made by dissolving lyophilized peptide in 1 mL of Nanopure water. Concentration was determined using the Edelhoch method [26]. In short, 5–10 μL of peptide stock was diluted in 1 mL of Nanopure water to get a UV absorbance between 0.1 to 1 absorbance unit at 280 nm. Absorbance of amino acid side chains, in this case, only tyrosine, at 276, 278, 280, and 282 nm was measured and the total concentration of peptide was determined using estimated extinction coefficients of tyrosine at these wavelengths [26]. Peptide stock solution was stored in sealed containers in a N_2 environment. Copper(II) stock solutions were prepared by dissolving copper sulfate (Cu(II)SO4, Sigma) in Nanopure water. Cu(II) stock solution was standardized by EDTA titration in an ammonium buffer to a murexide endpoint. Copper(I) stock solutions were prepared fresh daily by dissolving tetrakis(acetonirile)copper(I) hexafluorophosphate ($[Cu(CH_3CN)_4]PF_6$, Sigma-Aldrich) in anhydrous acetonitrile (Sigma-Aldrich) under a N_2 atmosphere using a Coy anaerobic chamber. Copper(I) stock solutions were standardized by titrating aliquots of stock solution into an excess of the chromophoric ligand anion bicinchoninate (BCA, Sigma) in degassed, Nanopure water.

Concentration was determined from the absorption of the $Cu(I)(BCA)_2$ complex ($\lambda_{max} = 562$ nm, $\varepsilon = 7900\ M^{-1}$) [27].

2.3. Preparation of Cu–peptide complexes

All solutions were generated at Cu:peptide ratio of 0.8:1, unless stated otherwise. Our peptide stock concentrations are determined using *estimated* [26] extinction coefficients, thus a 25% excess of peptide is deliberately added to Cu–peptide mixtures to avoid excess Cu(II) in solution. Peptide:copper stoichiometry is 1:1 in the solutions used here according to our previously published data [20].

Cu(II)–peptide complexes were generated by combining $Cu(II)SO_4$ stock solution with the peptide stock solution in Nanopure water buffered at pH 7.4 with 50 mM HEPES unless stated otherwise.

Cu(I)–peptide complexes were generated under anaerobic atmosphere in degassed Nanopure water. A stock solution of $[Cu(I)(CH_3CN)_4]PF_6$ was combined with the peptide stock solution, buffered at pH 7.4 with 50 mM HEPES unless stated otherwise.

2.4. Reaction of peptide–Cu(II) complex with ascorbate

A solution of L-ascorbic acid (prepared fresh daily) was added to buffered Cu(II)–peptide solutions (described above). Buffer concentration is at least 50 times excess of ascorbic acid added, and pH did not change significantly before and after the addition of ascorbic acid. Upon the addition of 1 mM ascorbic acid to 50 mM pH 7.4 buffer, ascorbate will predominate. In the case of oxygen-free reaction, peptide–Cu(II) and ascorbic acid solutions were degassed prior to mixing.

2.5. Anaerobic manipulations

Anaerobic reactions and manipulations were performed under N_2 atmosphere in a Coy anaerobic chamber ($O_2 < 3$ ppm) or with anaerobic cuvettes fitted with screw-cap septa, and degassed with N_2.

2.6. UV–vis spectroscopy

Absorption spectra were recorded in 1-cm quartz cuvettes on an SI Photonics (Tucson, AZ) model 420 fiber optic CCD array UV–vis spectrophotometer.

2.7. EPR spectroscopy

X-band electron paramagnetic resonance (EPR) data were acquired using quartz EPR tubes and a Bruker EMX spectrophotometer with the following parameters; frequency 9.43 GHz, modulation 0.5 mT, center field 310 mT, sweep width 150 mT, sweep time 30 s, receiver gain 30 dB, microwave power 0.2 mW. All the spectra were recorded at liquid nitrogen temperature and samples containing 10% (*v*/*v*) glycerol.

2.8. Cu K-edge X-ray absorption spectroscopy

Data were collected on beamline X3b at the National Synchrotron Light Source (Brookhaven National Laboratories; Upton NY). Samples were maintained at 25 K throughout data collection by the use of a closed cycle helium cryostat. Light was monochromatized using a Si(111) double crystal monochromator and focused with a low angle Ni mirror, which was also used for harmonic rejection. All data are reported as fluorescence data, which were collected using a Canberra 31 element solid-state Ge detector with a 3-μm thick Ni-foil filter placed between the detector and sample. Count rates were maintained under 25 kHz per channel. Energies were calibrated against the spectrum of a Cu-foil (first inflection point assigned to 8980.3 eV), which was recorded simultaneously during data collection. Data were collected in 5 eV steps from 200–20 eV below the edge (averaged over 1 s), 0.3 eV steps in the edge region (20 eV below the edge to 30 eV above the edge; averaged over 3 s), 2 eV steps from 30–300 eV above the edge (averaged over 5 s), and 5 eV steps from 300 eV above the edge to 14 *k* (averaged over 5 s). Although no photoreduction was observed, after every scan the X-ray beam was moved to an unexposed spot on the sample. The reported data represent the average of 10 individual data sets. Spectra from individual detector channels were inspected prior to data averaging, and known monochromator glitches were removed. Data were worked-up and modeled using *EXAFS123* [28] and FEFF 7.02 [29], as previously described [20,30]. Phase (α) and amplitude functions (f) and multiple scattering functions were constructed for both the Cu–imidazole$_2$ and Cu–imidazole moieties to isolate the *trans* imidazoles from the mono-imidazole. Refinements are based on unfiltered k^3 data over the range $k = 2$–$14\ Å^{-1}$.

3. Results

The series of $CtrA_n$ peptides based on the sequence of the first 14 amino acids of human Ctr1 were synthesized (Table 1). The native-sequence peptide, Ctr1-14, has been investigated previously [5,7,20]. This native-sequence peptide contains the ATCUN and *bis*–His motifs discussed above, which participate in Cu(II) acquisition from human serum albumin and copper reduction in the presence of ascorbate. Ctr1-14 also possesses a Mets-motif, but Mets-motifs in *human* Ctr1 are not the predominant Cu-binding motifs as they are in *yeast* Ctr1 [7,11,12,20]. In this study, we focused on the question of how sequence proximity between the ATCUN and *bis*–His motifs affect the ability of Ctr1 model peptides to facilitate copper reduction by ascorbate. To investigate this question, we synthetically varied the distance between that native ATCUN and *bis*–His motifs (underlined in Table 1) using 0–4 alanine insertions and tested each peptide's ability to reduce Cu(II) and stabilize Cu(I) in the presence of ascorbate, at pH 7.4, under ambient conditions (approximately 20% O_2).

3.1. Reaction of Cu(II)–peptide with ascorbate and dioxygen

Peptide–Cu(II) complexes were generated in HEPES buffer at pH 7.4 under ambient conditions. Each peptide in the $CtrA_n$ series displays a band at 525 nm with an extinction coefficient of 100 $M^{-1}\ cm^{-1}$ (Fig. 1). This band is characteristic of the 4N coordination environment of Cu(II) by the ATCUN motif, and indicates that all peptides in the $CtrA_n$ series coordinate Cu(II) in a similar coordination environment [9]. EPR spectroscopy data support the assignment of 4N ATCUN coordination, as is expected for Cu(II)–ATCUN (see supplementary information (SI), Fig. S1).

Upon the addition of 1 M equivalent of ascorbate, time-dependent changes in the UV–vis features are observed (Fig. 1). In the case of Cu(II)–Ctr1-14 complex (Fig. 1 A), the addition of ascorbate results in a steady decrease in the UV–vis absorption band at 525 nm, as reported previously under nearly identical conditions [7]. The Ctr1-14 peptide binds to both Cu(II) and Cu(I) with high affinity, therefore the decrease in the Cu(II)-ATCUN d–d band at 525 nm is indicative of Cu(II) reduction and formation of Cu(I)–peptide. The assumption that decrease in absorbance at 525 nm indicates formation of Cu(I)–peptide is further supported with EPR spectroscopy (see SI, Fig. S1).

It was previously determined that the *bis*–His motif in Ctr1-14 is required for reduction of Cu(II)–Ctr1-14, as observed in Fig. 1A. Since all peptides in the $CtrA_n$ series also possesses a *bis*–His motif, we initially expected that upon addition of ascorbate, a time-dependent decrease in the 525 nm Cu(II)–ATCUN feature would be observed for all $CtrA_n$ peptide–Cu(II) complexes. This is the case for two of the peptides (Fig. 1, C ($CtrA_1$) and D ($CtrA_2$)). However, a new feature begins to appear near 400 nm in the case of $CtrA_2$.

In contrast, very little change is observed in the UV–vis spectrum upon addition of ascorbate to solutions of the $CtrA_0$ peptide–Cu(II) complex (Fig. 1, B). This $CtrA_0$ peptide behaves as if the *bis*–His motif were not present and resembles previously-characterized ATCUN-only peptides in that the Cu(II)–ATCUN complex is not significantly reduced by

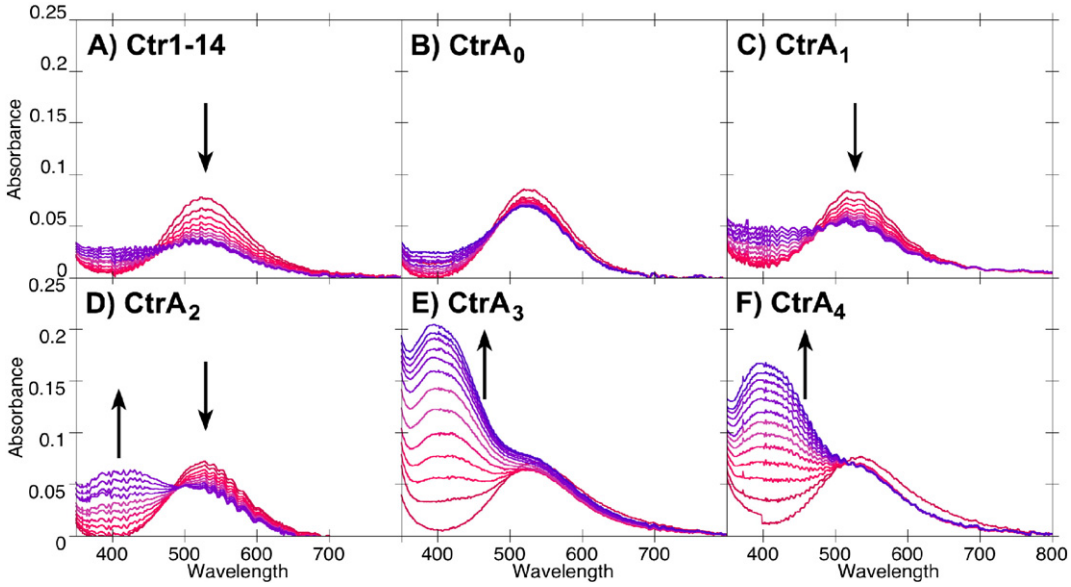

Fig. 1. Time-dependent UV–vis spectra of ascorbate reaction with Cu(II)–peptide complex under ambient conditions (20% O_2) and monitored over 1 h. Solutions are 1 mM peptide, 0.8 mM Cu(II), and 1 mM ascorbic acid, buffered at pH 7.4 with 50 mM HEPES under ambient atmosphere (20% O_2). Peptide sequences are shown in Table 1 and are labeled in this figure. All initial spectra at T = 0 have λ_{max} at 525 nm, indicating Cu(II)–ATCUN 4N coordination. Changes in spectra upon addition of ascorbate are indicated with arrows.

ascorbate [7,21]. In the case of the $CtrA_3$ and $CtrA_4$ peptides, the initial reduction is observed in the Cu(II)–ATCUN band at 525 nm, followed by the appearance of the new feature near 400 nm (Fig. 1, E ($CtrA_3$) and F ($CtrA_4$). Control experiments were done under excess peptide and different buffer conditions to ensure that the features observed near 400 nm were not a result of excess copper in solution or due to side-reactions of the HEPES buffer, and to demonstrate that the species corresponding to the 400 nm band is due to the copper–peptide complex (SI, Figs. S2 and S3).

Ascorbate-mediated reductions of the $CtrA_n$–copper complex under similar conditions, yet in anaerobic atmosphere, demonstrate that formation of the species producing the 400 nm band is O_2-dependent (SI, Fig. S4). The species corresponding to the 400 nm band are, however, produced under anaerobic conditions in the case that both ascorbate and H_2O_2 are present (SI, Fig. S4). The species contributing to absorbance near 400 nm is also acid-labile (SI, Fig. S5). These observations are all characteristic of Cu(II)–peptide complexes which react through intermediates involving Cu(III) contained within ACTUN-like environments [21,31–34].

Margerum and coworkers have shown that Cu(II)–ATCUN complexes can undergo reaction with a combination of ascorbate and H_2O_2 to produce Cu(III)–ATCUN peptides. The spectral changes shown in Fig. 1E are strikingly similar to those reported for Cu(III)–peptides. These Cu(III)–peptide intermediates give intense absorption at 396 nm and undergo rapid oxidative degradation to form α-hydroxyhistidyl peptides, which dehydrate to form α,β-dehydrohistidyl peptide derivatives [21, 32]. The Cu(II) complexes of dehydrated peptide derivatives have intense absorptions between 430 and 460 nm [21], but absorption features of α-hydroxyhistidyl peptides bound to Cu(II) are not reported.

We analyzed the metallopeptide-based oxidation products using ultra-high performance liquid chromatography, tandem photodiode array, tandem mass spectrometry (UPLC–PDA-MS) following the reaction of the $CtrA_n$–copper metallopetides with ascorbate under aerobic conditions in order to determine the nature of the species absorbing near 400 nm (Fig. 1) in our reaction solutions. Upon the separation and subsequent analysis of reaction products by UPLC–PDA-MS, we identified a species having the mass of Cu(II)–peptide plus oxygen, indicative of the oxidized metallopeptide (SI, Fig. S6). This species has a strong UV–vis absorbance at 412 nm and a weaker absorbance at 520 nm. Under acidic conditions, Cu(II) coordination is lost and a species consistent with the mass of peptide plus oxygen was observed with strong absorbance at 390 nm. We conclude from these data (see SI, Fig. S6) that the band near 400 nm, observed in Fig. 1 indicates oxidative damage to the peptide. These results are consistent with the oxidation of the peptide through the initial generation of Cu(III) intermediates. Unlike other reports [21,31,32], we did not observe alkene peptide products in our UPLC–PDA-MS results. We did, however, observe minor amounts of peptide species with multiple additions of oxygen. These products had similar absorbance spectra to the mono-oxidized peptide (SI, Fig. S6).

Fig. 1 shows that reactivity of Cu(II)–peptide with ascorbate under ambient conditions depends on the sequence proximity between the *bis*–His and ATCUN motifs. The $CtrA_0$ gives no observable change in Cu(II) oxidation state. $CtrA_2$ and $CtrA_3$ peptides produce a distinct band near 400 nm, indicating O_2-dependent oxidative damage to the peptide. A significant observation is that peptides which retain the native sequence Ctr1 spacing of 1 amino acid between ATCUN and *bis*–His are able to facilitate the reduction of Cu(II) to Cu(I), stabilize Cu(I) under aerobic conditions, and also may protect the peptide from oxidative damage.

3.2. Sequence-dependent changes in Cu(I) structure

The difference in reactivity observed here among the $CtrA_n$ series Cu(II)–peptide complexes may be explained by structural differences in copper binding sites, specifically differences among the Cu(I) binding sites of each peptide. We focused on comparing the Cu(I) structure of two peptides that represent opposite ends of the spectrum of reactivity: Ctr1-14, which best stabilizes the Cu(I) oxidation state, and $CtrA_3$, which produced the greatest degree of aerobic oxidative damage following the reduction of the copper center.

The structure of Cu(I) binding to Ctr1-14 model peptide was recently reported as a N_2OS coordination site [20]. However, XAS studies of the Cu(I) bound to the $CtrA_3$ peptide demonstrate that it contains Cu(I) in a coordination environment that is distinct from the Cu(I) adduct of Ctr1-14. The XANES region of the Cu K-edge X-ray absorption spectrum of Cu(I)–$CtrA_3$ is consistent with a three coordinate distorted T-shaped environment about Cu(I). Analysis of the EXAFS region of the Cu K-edge spectrum supports this formulation (Fig. 2). The data is best modeled with two imidazole N-atom donors at 1.99 Å, which are *trans* to one

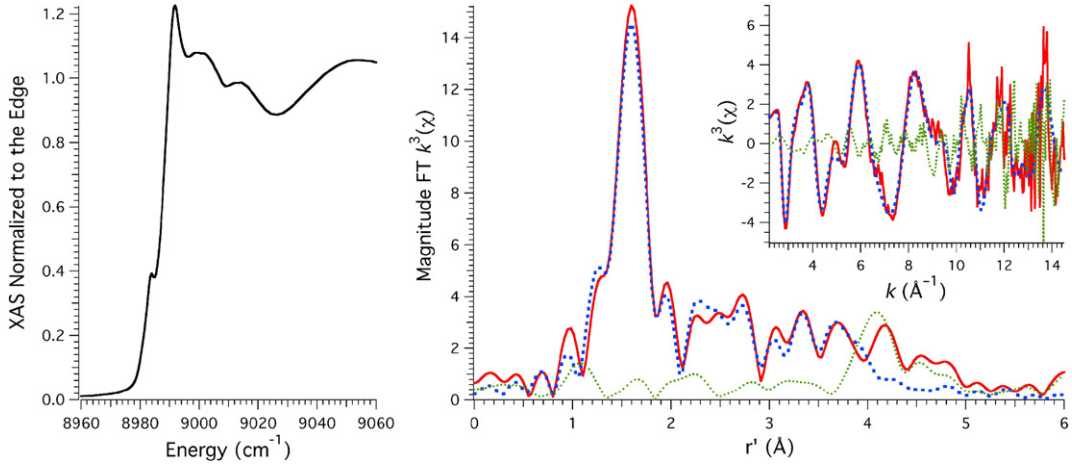

Fig. 2. Left: XANES region of the Cu K-edge XAS spectrum of Cu(I)–CtrA$_3$. Right: Magnitude Fourier Transformed k^3 EXAFS spectrum of Cu(I)–CtrA$_3$ depicting the experimental data (red solid spectrum), simulation to the EXAFS data (dashed blue spectrum), and difference spectrum (dotted green spectrum). Inset: k^3 EXAFS spectrum of Cu(I)–CtrA$_3$ depicting the experimental data (red solid spectrum), simulation to the EXAFS data (dashed blue spectrum), and difference spectrum (dotted green spectrum). EXAFS simulation parameters — Shell 1 (*bis*–imidazole): n = 1, r = 1.987(2) Å, and σ^2 = 0.003(2) Å^{-1}; Shell 2 (imidazole): n = 1, r = 2.042(4) Å, and σ^2 = 0.004(2) Å^{-1}; and ε^2 = 1.11.

another, and a longer imidazole N-atom donor at 2.04 Å. Thus, the addition of the three Ala spacer between H3 and H5 dramatically alters the coordination geometry about Cu(I). In the case of CtrA$_3$, the methionine ligand has been lost, while all three histidine residues are now coordinated to the Cu(I)-center (Fig. 3).

The two Cu(I) coordination environments in Ctr1 and CtrA$_3$ are predicted to demonstrate different reactivity with O_2 due to differences in coordinate bond covalencies and steric bulk about the Cu(I) center [36,37]. The 4-coordinate quasi tetrahedral N_2OS center of Ctr1-14 is expected to be less reactive with O_2 than the distorted T-shaped 3N coordination provided by CtrA$_3$. As part of our analysis, we examined the relative behavior of Cu(I)–peptide complexes upon exposure to ambient atmosphere (~20% O_2). The Cu(I)–CtrA$_3$ complex oxidized completely to Cu(II)–CtrA$_3$ within 20 min of standing in ambient atmosphere, where the Ctr1-14 peptide became fully oxidized after approximately 2 h (SI, Fig. S7).

4. Discussion

The amino-terminal domain of human Ctr1 contains two important histidine motifs that are involved in acquiring and reducing copper prior to transport through the Ctr1 pore. The Ctr1 ATCUN motif, described above, enables Ctr1 to thermodynamically compete for Cu(II) with human serum albumin. In fact, both Ctr1 and human serum albumin proteins contain ATCUN sites with similar thermodynamic binding constants for Cu(II) (approximately 1 pM affinity) [7,38]. Cu(II) bound at

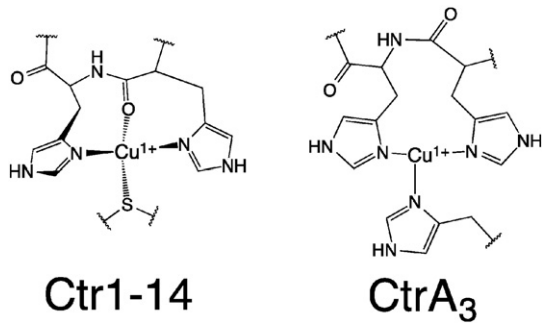

Fig. 3. Left: The structure of Cu(I) bound to Ctr1-14 [20] is 4-coordinate N_2OS with quasi tetrahedral geometry. Right: Structure of Cu(I) bound to CtrA$_3$ peptide is 3N(imidazole) with distorted T-shaped geometry.

the ATCUN site in Ctr1 peptides can be reduced by ascorbate and transferred to an alternate site comprised of two adjacent histidines (*bis*–His) and one methionine. This binding site has a high affinity for Cu(I) (0.1 pM affinity). It is noted that the presence of the *bis*–His is required for copper reduction. Upon reduction, Ctr1 peptides form relatively stable peptide–Cu(I) species, even under aerobic conditions [7].

Here we investigated the CtrA$_n$ series of model peptides. Each of the CtrA$_n$ peptides coordinates Cu(II) using the high-affinity ATCUN motif. Alteration of the proximity between the ATCUN and *bis*–His motifs results in a spectrum of reactivity. Upon the reaction with ascorbate under aerobic conditions, Cu(II) complexes of the native-sequence Ctr1-14 peptide and the CtrA$_1$ peptide facilitate the reduction of copper and form Cu(I)–peptide complexes. Variations in the one amino acid spacing between the ATCUN and *bis*–His motifs yield differential Cu(II) reactivity. Elimination of the spacing between the ATCUN and *bis*–His motifs (CtrA$_0$) prevents the reduction of the Cu(II)–metallopeptide complex. Increasing the spacing between the ATCUN and *bis*–His motifs (CtrA$_2$–CtrA$_4$) results in the oxidative damage of the peptide.

The mechanism by which ascorbate and dioxygen or hydrogen peroxide ultimately oxidize the peptide is uncertain. Oxidation of peptide may occur as a result of Cu(III) intermediates, which then degrade by mechanisms reported by McDonald and coworkers to form oxidized peptide products [35]. Cu(III) intermediates could be produced by either one-electron oxidation of Cu(II) by peroxide, as reported by Mylonas and coworkers [33], or by two-electron oxidation of Cu(I). Alternatively, the reaction of Cu(I) with oxygen species may produce reactive oxygen species which subsequently oxidize peptides. The production of reactive oxygen species by oxidation of Cu(I) is not mutually exclusive with the production of Cu(III) species.

All peptides in the CtrA$_n$ series coordinate Cu(II) similarly through ATCUN coordination according to UV–vis and EPR data (Figs. 1 and S1), but this fact does not preclude involvement of distal axial ligands or secondary coordination sphere differences, which may affect Cu(II) reactivity. Alternatively, differential structure of the reduced Cu(I) centers in various peptides could influence reactivity with O_2. We have shown that Cu(I) coordination is significantly influenced by the variation in sequence between the two cases of Ctr1-14 and CtrA$_3$ peptides. Therefore, differences in Cu(I) structure may explain differences in metallopeptide reactivity.

In the case of the CtrA$_0$ peptide, lack of metallopeptide reduction is likely due to the inability of the two histidine imidazoles to effectively coordinate to the copper center and subsequently stabilize the

Cu(I) oxidation state. In contrast, the $CtrA_2$–$CtrA_4$ peptides, with the greater degree of flexibility between the ACTUN and *bis*–His motifs allow for the 3N coordination environment about Cu(I), which subsequently promotes O_2 reactivity. It is only in the peptides with the one amino-acid spacing between the ACTUN and *bis*–His motif that Cu(I) can be both generated and stabilized.

The specific relationship between ATCUN and *bis*–His motifs in human Ctr1 model peptide facilitates Cu(II) reduction by ascorbate and stabilizes Cu(I), thus protecting against reaction with O_2. We propose that Ctr1 methionine coordination in the native sequence prevents 3N coordination and forces a quasi-tetrahedral environment, with one methionine ligand, that is critical in preventing bound Cu(I) from reacting with O_2, and preventing oxidative damage to the peptide. Met thioether coordination likely stabilizes the Cu(I) oxidation state within Ctr1 as it yields a soft donor to the soft Cu(I) Lewis acid center. These data therefore suggest that specific patterns of combined methionine and histidine amino acids act as modulators of copper redox chemistry.

Alteration of the proximity between the ATCUN and *bis*–His motifs results in a spectrum of reactivity ranging from no change in the Cu(II)–ATCUN complex to formation of either stable Cu(I)–peptide species or reactive species that subsequently result in oxidative damage to the peptide. It is apparent from this work that a sequence spacing of one amino acid between ATCUN and *bis*–His is ideal for meeting the reductase-like and copper-transport requirements of Ctr1. The specific relationship between ATCUN and *bis*–His motifs in human Ctr1 model peptide facilitates Cu(II) reduction by ascorbate and stabilizes Cu(I) while protecting against oxidation of the peptide. Variation of the native Ctr1 spacing between ATCUN and *bis*–His in the $CtrA_n$ series studied here reveals that reductase properties can be lost and/or aberrant oxidative chemistry can result.

These data therefore demonstrate that the amino acid sequence can be used to tune the Cu redox chemistry, ranging from net reduction to net oxidation of the metallopeptide complex. Histidine and methionine sequences are a major determining factor governing the ultimate fate of Cu–peptide complexes upon reaction with biological reducing agent (ascorbate) and oxidizing agent (O_2). This paper represents our first steps toward understanding how amino acid sequence controls Cu redox chemistry, with important implications in the biological trafficking and reactivity of copper.

5. Associated content

5.1. Supplementary information

EPR Spectra of Cu(II)–$CtrA_n$ series and of Cu(II)–Ctr1-14 and Cu(II)–$CtrA_3$ reaction with ascorbate, ascorbate-dependent reduction of 2:1 peptide:Cu and 1:1 peptide:Cu in phosphate buffer, dependence of reaction products on O_2 and H_2O_2, acid-sensitivity of 400 nm species, UPLC–PDA-MS analysis of reaction products, and sequence-dependent rate of Cu(I)–peptide oxidation.

Author contributions

The manuscript was written through contributions of all authors. All authors have given approval to the final version of the manuscript.

Abbreviations

ATCUN	amino terminal Cu(II) and Ni(II) binding site, this motif is comprised of a histidine in the third position from a free amino terminus
bis-His	HisHis or HH sequence (two adjacent histidines)
Ctr1	copper transporter 1
Ctr1-14	peptide sequence based on the first fourteen amino acids of human Ctr1: MDHSHHMGMSYMDS
$CtrA_n$	series of peptides based on Ctr1-14, but where varying number of alanine amino acids replace Ser 4 and separate the ATCUN and *bis*–His motifs with n = 0–4 alanines (see Table 1 for sequences).

Acknowledgments

We thank Dr. Graham Lappin, for enlightening conversations about Cu(III)-peptide chemistry. We thank Dr. Katherine Franz for critical access to instrumentation and for fruitful discussions that motivated this manuscript. We are grateful to Dr. Chris Dunlap for the consultation and instrument support at Saint Mary's College and to Ms. Claire R. Bleecker, Dr. Dorothy Feigl, Dr. James Parise, and Dr. Jake Pushie for the assistance in editing this manuscript. K.L.H acknowledges financial support from the Lilly New Faculty Scholars Program (Lilly Endowment Inc, 2004-1871-000), Saint Mary's College, the Center for Academic Innovations 2013 Faculty Development Research Grant, and the 2014 Maryjean R. Burke and Daughters SISTAR award. S.E.C. acknowledges support from the US National Institutes of Health (NIH; GM084176 SUB-P2033195). J.S acknowledges financial support from the National Science Foundation (CHE-1362662). All X-ray absorption studies were performed at the NSLS. The use of the National Synchrotron Light Source, Brookhaven National Laboratory, was supported by the US Department of Energy, Office of Science, Office of Basic Energy Sciences, under Contract no. DE-AC02-98CH10886. Cu K-edge studies were preformed on beamline X3-b, which is supported through the Case Center for Synchrotron Biosciences, which is funded through the National Institute of Biomedical Imaging and Bioengineering (NIH Grant no. P30-EB-009998).

Appendix A. Supplementary data

Supplementary data to this article can be found online at http://dx.doi.org/10.1016/j.jinorgbio.2015.12.021.

References

[1] H. Ohrvik, D.J. Thiele, S. New York Acad, Ann. N.Y. Acad. Sci. 1314 (2014) 32–41.
[2] N.K. Wee, D.C. Weinstein, S.T. Fraser, S.J. Assinder, Int. J. Biochem. Cell Biol. 45 (2013) 960–963.
[3] R.A. Festa, D.J. Thiele, Curr. Biol. 21 (2011) R877–R883.
[4] M.M.O. Pena, J. Lee, D.J. Thiele, J. Nutr. 129 (1999) 1251–1260.
[5] Y. Shenberger, A. Shimshi, S. Ruthstein, J. Phys. Chem. B 119 (2015) 4824–4830 (American Chemical Society).
[6] X.B. Du, H.Y. Li, X.H. Wang, Q. Liu, J.Z. Ni, H.Z. Sun, Chem. Commun. (Cambridge, U. K.) 49 (2013) 9134–9136.
[7] K.L. Haas, A.B. Putterman, D.R. White, D.J. Thiele, K.J. Franz, J. Am. Chem. Soc. 133 (2011) 4427–4437 (American Chemical Society).
[8] R. Sankararamakrishnan, S. Verma, S. Kumar, Proteins 58 (2005) 211–221.
[9] C. Harford, B. Sarkar, Acc. Chem. Res. 30 (1997) 123–130.
[10] J.T. Rubino, K.J. Franz, J. Inorg. Biochem. 107 (2012) 129–143.
[11] J.T. Rubino, P. Riggs-Gelasco, K.J. Franz, J. Biol. Inorg. Chem. 15 (2010) 1033–1049.
[12] J.F. Jiang, I.A. Nadas, M.A. Kim, K.J. Franz, Inorg. Chem. 44 (2005) 9787–9794.
[13] E. Georgatsou, L.A. Mavrogiannis, G.S. Fragiadakis, D. Alexandraki, J. Biol. Chem. 272 (1997) 13786–13792.
[14] J. Lee, M.M.O. Pena, Y. Nose, D.J. Thiele, J. Biol. Chem. 277 (2002) 4380–4387.
[15] S.G. Aller, V.M. Unger, Proc. Natl. Acad. Sci. U. S. A. 103 (2006) 3627–3632.
[16] C.J. De Feo, S.G. Aller, G.S. Siluvai, N.J. Blackburn, V.M. Unger, Proc. Natl. Acad. Sci. U. S. A. 106 (2009) 4237–4242.
[17] R. Hassett, D.J. Kosman, J. Biol. Chem. 270 (1995) 128–134.
[18] I.F. Scheiber, J.F.B. Mercer, R. Dringen, Neurochem. Int. 56 (2010) 451–460.
[19] J. Lee, M.J. Petris, D.J. Thiele, J. Biol. Chem. 277 (2002) 40253–40259.
[20] M.J. Pushie, K. Shaw, K.J. Franz, J. Shearer, K.L. Haas, Inorg. Chem. 54 (2015) 8544–8551.
[21] S.K. Burke, Y.L. Xu, D.W. Margerum, Inorg. Chem. 42 (2003) 5807–5817.
[22] S. Melino, C. Santone, P. Di Nardo, B. Sarkar, FEBS J. 281 (2014) 657–672.
[23] W.M. Tay, A.I. Hanafy, A. Angerhofer, L.J. Ming, Bioorg. Med. Chem. Lett. 19 (2009) 6709–6712.
[24] Y. Bouter, K. Dietrich, J.L. Wittnam, N. Rezaei-Ghaleh, T. Pillot, S. Papot-Couturier, T. Lefebvre, F. Sprenger, O. Wirths, M. Zweckstetter, T.A. Bayer, Acta Neuropathol. 126 (2013) 189–205.
[25] E. Portelius, N. Bogdanovic, M.K. Gustavsson, I. Volkmann, G. Brinkmalm, H. Zetterberg, B. Winblad, K. Blennow, Acta Neuropathol. 120 (2010) 185–193.
[26] C.N. Pace, F. Vajdos, L. Fee, G. Grimsley, T. Gray, Protein Sci. 4 (1995) 2411–2423.

[27] Z. Xiao, F. Loughlin, G.N. George, G.J. Howlett, A.G. Wedd, J. Am. Chem. Soc. 126 (2004) 3081–3090 (American Chemical Society).
[28] J. Shearer, R.C. Scarrow, University of Nevada, Reno, NV, 2015.
[29] S.I. Zabinsky, J.J. Rehr, A. Ankudinov, R.C. Albers, M.J. Eller, Phys. Rev. B 52 (1995) 2995–3009.
[30] J. Shearer, V.A. Szalai, J. Am. Chem. Soc. 130 (2008) 17826–17835.
[31] D.W. Margerum, K.L. Chellappa, F.P. Bossu, G.L. Burce, J. Am. Chem. Soc. 97 (1975) 6894–6896 (American Chemical Society).
[32] M.R. McDonald, F.C. Fredericks, D.W. Margerum, Inorg. Chem. 36 (1997) 3119–3124.
[33] M. Mylonas, G. Malandrinos, J. Plakatouras, N. Hadjiliadis, K.S. Kasprzak, A. Krezel, W. Bal, Chem. Res. Toxicol. 14 (2001) 1177–1183.
[34] P. Kaczmarek, M. Jezowska-Bojczuk, K. Gatner, W. Bal, Dalton Trans. (2005) 1985–1988.
[35] M.R. McDonald, W.M. Scheper, H.D. Lee, D.W. Margerum, Inorg. Chem. 34 (1995) 229–237 (American Chemical Society).
[36] E.I. Solomon, D.E. Heppner, E.M. Johnston, J.W. Ginsbach, J. Cirera, M. Qayyum, M.T. Kieber-Emmons, C.H. Kjaergaard, R.G. Hadt, L. Tian, Chem. Rev. 114 (2014) 3659–3853.
[37] E.I. Solomon, R.G. Hadt, Coord. Chem. Rev. 255 (2011) 774–789.
[38] M. Rózga, M. Sokołowska, A. Protas, W. Bal, J. Biol. Inorg. Chem. 12 (2007) 913–918.